RADIATION MAPPING ON SPACELAB 1:
EXPERIMENT NO. INS006
FINAL REPORT

E. V. Benton
Principal Investigator

Co-Investigators: A. Frank, R. Cassou, R. Henke and V. Rowe

(NASA-CR-171893) RADIATION MAPPING ON SPACELAB 1: EXPERIMENT NO. INS006 Final Report (San Francisco Univ.) 24 p HC A02/MF A01 CSCL 22B

N86-15332

Unclas
G3/16 29017

1 March 1985
USF Technical Report No. 68
Prepared under Contract No. NAS9-15337
at the

Physics Research Laboratory
University of San Francisco
San Francisco, California 94117

*Work supported by NASA-Lyndon B. Johnson Space Center, Houston, Texas 77058.

RADIATION MAPPING ON SPACELAB 1:
EXPERIMENT NO. INS006

Abstract — The report describes the first attempt at mapping the radiation environment inside Spacelab. Measurements were made by a set of passive radiation detectors distributed throughout the volume inside the Spacelab-1 module, in the access tunnel and outside on the pallet. Measurements of the low LET (linear energy transfer) component obtained from the TLD (thermoluminescent detectors) ranged from 92 to 134 mrad, yielding an average low LET dose rate of 10.0 mrads/day inside the module, which is about twice the low LET dose rate measured on previous flights of the Space Shuttle. Because of the higher inclination orbit (57° vs. 28.5° for previous STS flights), substantial fluxes of highly ionizing HZE particles (high charge and energy galactic cosmic rays) were observed for the first time on an STS flight, yielding an overall average mission dose-equivalent of 295 mrem, or 29.5 mrem/day, which is about three times higher than that measured on previous STS missions. Little correlation was found between measured average dose rates or HZE fluences and the estimated shielding throughout the volume of the module. The findings help to focus attention on the future problems of the space radiation environment for long-term human habitation, biomedical experimentation, and the design of the space station.

INTRODUCTION

The radiation encountered aboard spacecraft in Earth orbit is complex, both in particle type and energy spectra. This reflects the diverse origins of the radiation. There are primary galactic and solar components, either directly incoming or trapped within the radiation belts. These produce secondaries such as recoil nuclei, nuclear reaction products and bremsstrahlung through interaction with the materials of the spacecraft and its cargo. The fluxes and energy spectra are dependent on altitude and inclination of the orbit, on solar conditions, and amount, type and placement of shielding materials on the spacecraft.

For the orbits of the Spacelab-1 mission (STS-9) and the other space shuttle flights, the largest component of the radiation is from the energetic trapped protons. The HZE particles yield a smaller but significant component of dose equivalent, depending on the orbit inclination. In high altitude orbits, such as the geosynchronous orbit, trapped electrons become important. The radiation hazard from large solar flare events becomes significant as the spacecraft orbits are increased in altitude and inclination and the geomagnetic shielding is correspondingly reduced /1/. This is the case for orbits of inclination greater than $\sim 50^{\circ}$, polar and geosynchronous missions. Here, and particularly during extravehicular activity, potentially lethal doses of protons can be encountered. Also, for these orbits, substantial fluxes of high LET events from the HZE particles will be experienced. In addition to these naturally occurring radiations, orbiting spacecraft may encounter trapped electrons from high altitude nuclear tests as well as gamma rays and neutrons from on-board auxiliary power sources.

The ever-present radiation in the space environment may prove to be the single most important constraint on long-term manned space activities. The highly penetrating nature of some components of the space radiation field makes it impractical to provide enough shielding to the crew to completely eliminate the hazard. An indirect hazard also comes about from the effects of radiation on materials and electronics, in addition to the soft errors produced in computers. Biomedical experiments performed in space may need to take possible radiation effects into account. To date, only very limited experimental data exist on the radiation levels and the variation of these levels inside orbiting spacecraft /2-6/. Although computer codes have been developed for calculating the environment inside the orbiting spacecraft in specific orbits, a number of uncertainties exist including those in the proton models (about a factor of 2), in the electron belt models (about a factor of 5), in fragmentation cross-sections of heavy ions, etc. /7, 8/. Moreover, the shielding at any one location within the spacecraft is only approximately known and may vary as the crew and equipment are moved about, consumables used up, and the orientation of the spacecraft changes. The question of shielding poses one of the most difficult problems to solve in assessing radiation measurements; therefore it is essential to record these measurements at specific locations inside the spacecraft in addition to the dose received by the crew.

EXPERIMENT

The mapping of radiation levels throughout the spacecraft was performed with two detector types. There were 26 Passive Dosimeter Packets (PDP's) and four Thick Plastic Stack (TPS) packets. The PDP's had dimensions of 8.6 cm x 6.6 cm x 0.2 cm and each contained a set of Types 200 and 700 TLD detectors for the overall measurement and two layers of 1 mm-thick CR-39 plastic nuclear track detectors for the HZE particle measurement. Of these, 23 were deployed in the spacecraft and three remained on the ground as controls. The TPS's had dimensions of 9.8 cm x 9.8 cm x 5.2 cm and contained TLD's, CR-39 and AgCl crystals. The AgCl detectors provide information on the fragmentation of galactic cosmic rays passing through spacecraft shielding as well as a better characterization of the directionality of the radiation field at given detector locations.

The detectors were distributed over the inner surfaces of the Spacelab vehicle and the tunnel connecting to the crew compartment. The 26 locations represent a wide range of angular shielding distributions. The comparison of doses and HZE fluences at the different locations with the respective shielding at the sites yields important information on shielding effectiveness. The angular shielding distributions about the 23 PDP flight locations have been calculated for 512 equal solid angle bins /9/. These distributions are used in the comparisons.

A sketch of the Shuttle cargo bay is given in Figure 1, showing the locations of four PDP's at the Spacelab module end cones and two PDP's in the transfer tunnel. PDP's were also placed along the length of the module in sets of three as shown in Figure 2, where a sketch of the module cross section at racks 11 and 12 is given. The sets of three are spaced around the periphery of the module at five longitudinal distances. They are distributed at approximately equal radial angles, as in Figure 2, but the angles are rotated with respect to the module structure. Of the TPS's, two were forward in the module at opposite sides and one was at the middle of the module.

DATA

The TLD data has been analyzed and the CR-39 detectors from the PDP's have been processed and scanned for HZE particle fluences. Track measurements have also been made in order to obtain high LET (high specific ionization) particle spectra.

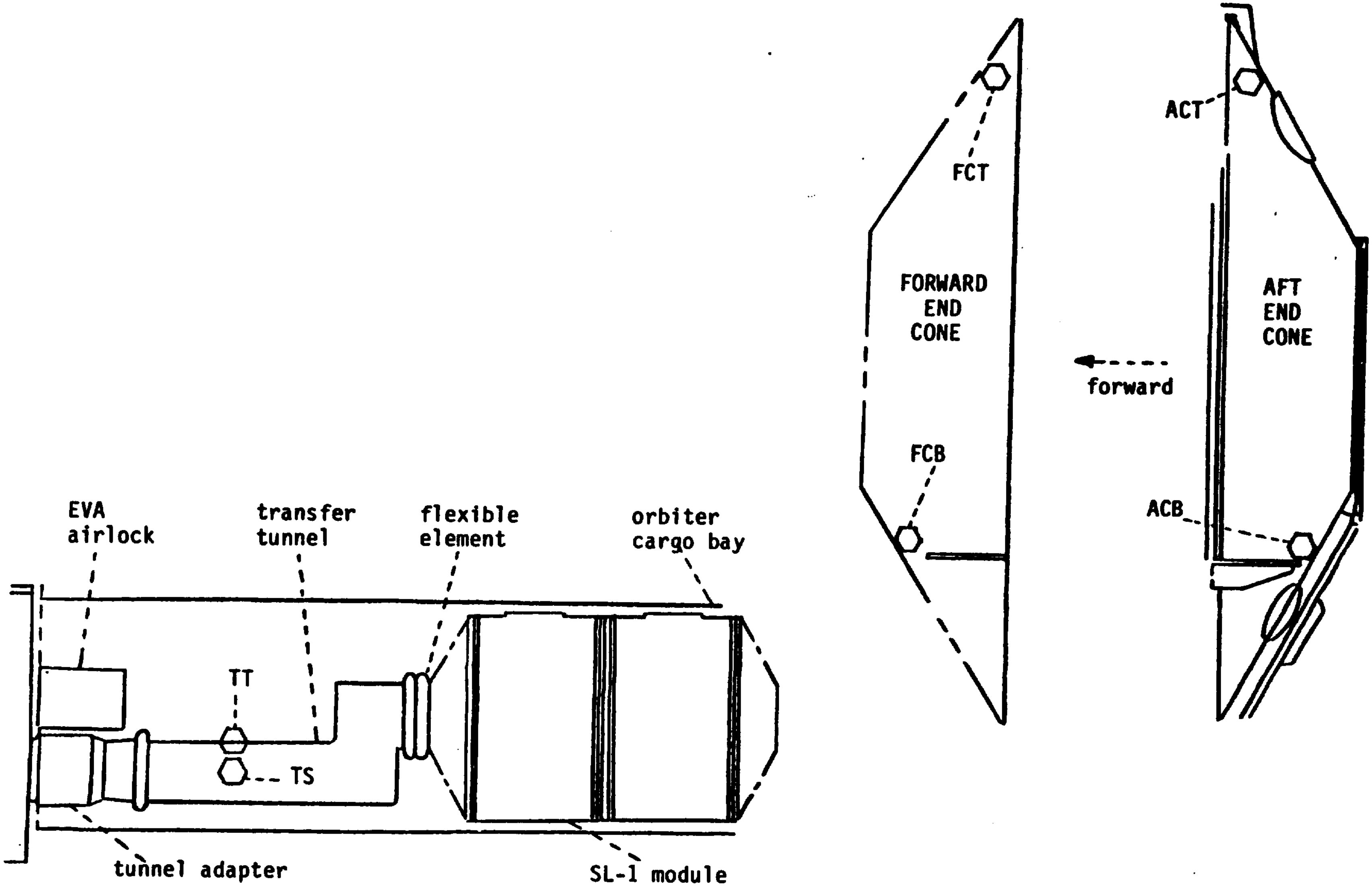

Fig. 1. Sketches of the positions of the SL-1 module and transfer tunnel in the cargo bay and of the module end cones, with the locations of PDPs TT, TS, FCT, FCB, ACT and ACB.

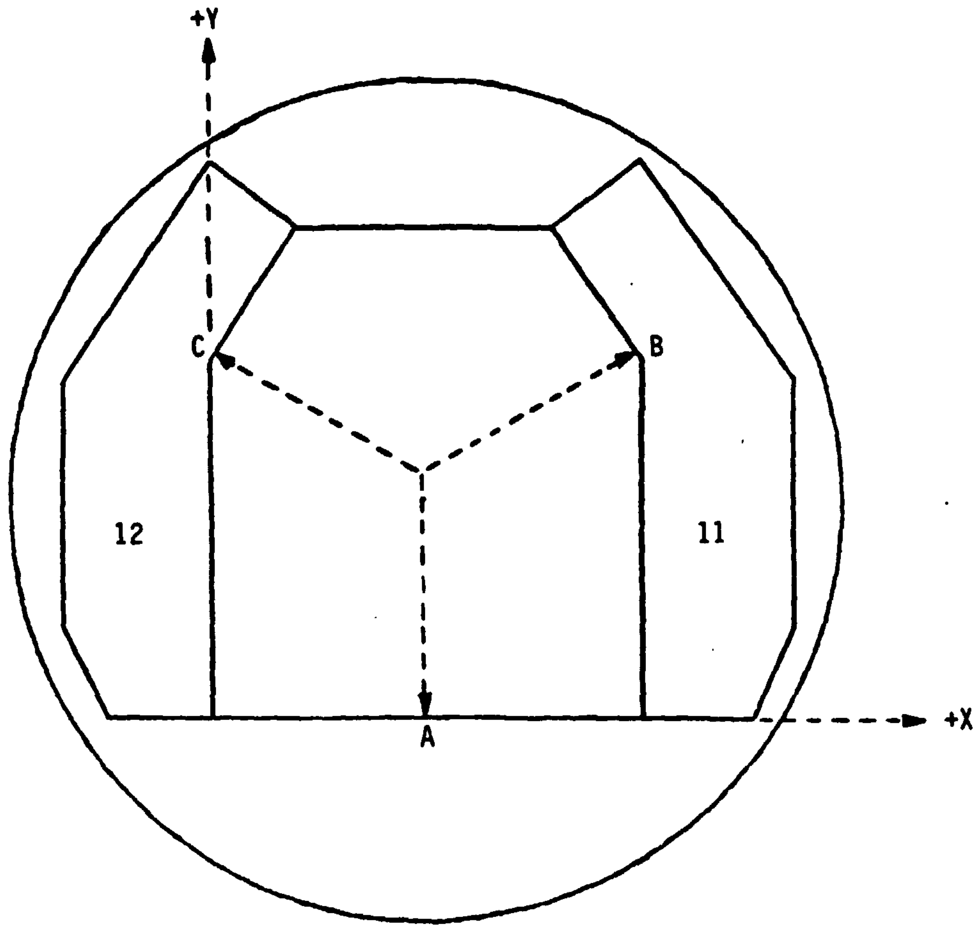

Fig. 2. Sketch of the view looking aft in the SL-1 module at racks 11 and 12. The positions of PDPs A, B and C are denoted, as are the positive X and Y directions. The X, Y coordinates of the three PDPs are (1069, 0), (2107, 1813) and (32, 1813), respectively.

In Table 1 is listed the TLD-700 dose in mrads and the observed fluence of HZE particles as a function of spacecraft location. The overall absorbed dose varied from ∿100 to 143 mrad inside the SL module. The observed HZE particle fluence varied from 154 to 435 tr/cm^2 in CR-39 for particles with LET$_\infty$ in water greater than ∿48 keV/μm /10/. The correlation between dose and HZE fluence is poor, as seen in Figure 3, where the two values have been plotted against each other for all the PDP's. Most of the TLD doses fall in the region from 100 to 115 mrads while the track fluences vary by a factor of 2.5 for these detectors. The two highest doses were recorded at the tops of the forward and aft end cones, which suggests less shielding at these sites. However, only the forward detector also had a higher-than-average number of HZE tracks.

The integral angular shielding distributions are plotted in Figures 4a and 4b for a selection of PDP's. Those selected range from the least to most heavily shielded. A comparison of the shielding curves with the corresponding TLD doses and HZE fluences in Table 1 discloses little correlation. The highest TLD doses were recorded by detectors which were among the least shielded, but the trend is not consistent. This can be seen in Figure 5 where the TLD doses have been plotted against the average shielding thicknesses. Without the two highest dose values, the profile of the measurements would be nearly flat. This plot is repeated in Figure 6 for the HZE track fluences. The scatter of the measured values is very large. In both figures the standard deviations about the linear regression lines and the correlation coefficients demonstrate the poor fitting.

The TLD doses and HZE particle fluences have also been plotted against the magnitudes of the less shielded ($\leq$ 12 g/cm^2) portions of the PDP solid angles in Figures 7 and 8. The value of 12 g/cm^2 was selected as a convenient cutoff for

TABLE 1. RADIATION MEASUREMENT ABOARD SPACELAB 1*

Detector location	TLD dose (mrad)	Observed HZE track fluence (cm^{-2})
PORT SIDE		
B	113.8 ± 6.1	367 ± 55
D	106.6 ± 4.0	297 ± 47
G	103.5 ± 3.4	154 ± 20
I	110.8 ± 3.4	250 ± 36
L	106.4 ± 2.7	326 ± 45
N	107.0 ± 4.8	211 ± 28
O	104.1 ± 2.8	313 ± 50
P	105.1 ± 3.8	167 ± 25
STARBOARD SIDE		
C	111.0 ± 3.3	305 ± 45
E	106.3 ± 3.7	380 ± 53
F	106.9 ± 4.5	349 ± 38
H	109.2 ± 3.7	167 ± 25
J	109.7 ± 2.6	391 ± 58
K	104.3 ± 3.1	161 ± 20
M	107.9 ± 4.0	292 ± 47
SL-1 FLOOR		
A	105.8 ± 2.6	292 ± 47
Q	104.0 ± 2.8	216 ± 28

Detector location	TLD dose (mrad)	Observed HZE track fluence (cm^{-2})
AFT END CONE		
ACT	141.0 ± 8.7	266 ± 41
ACB	102.5 ± 3.5	286 ± 39
FORWARD END CONE		
FCB	102.2 ± 2.7	245 ± 36
FCT	142.9 ±10.9	435 ± 59
SL-1 TUNNEL		
TS	122.3 ± 7.2	245 ± 36
TT	117.0 ± 4.5	286 ± 39
TPS MEASUREMENTS		
PORT FORWARD		
FCR	102.0 ± 2.6	
STARBOARD FORWARD		
FCL	102.3 ± 4.1	
MIDDLE OF SPACELAB		
DC	100.4 ± 1.5	

*The uncertainties shown are those due to counting statistics only; systematic errors resulting from a variety of factors may be as large as ± 30%.

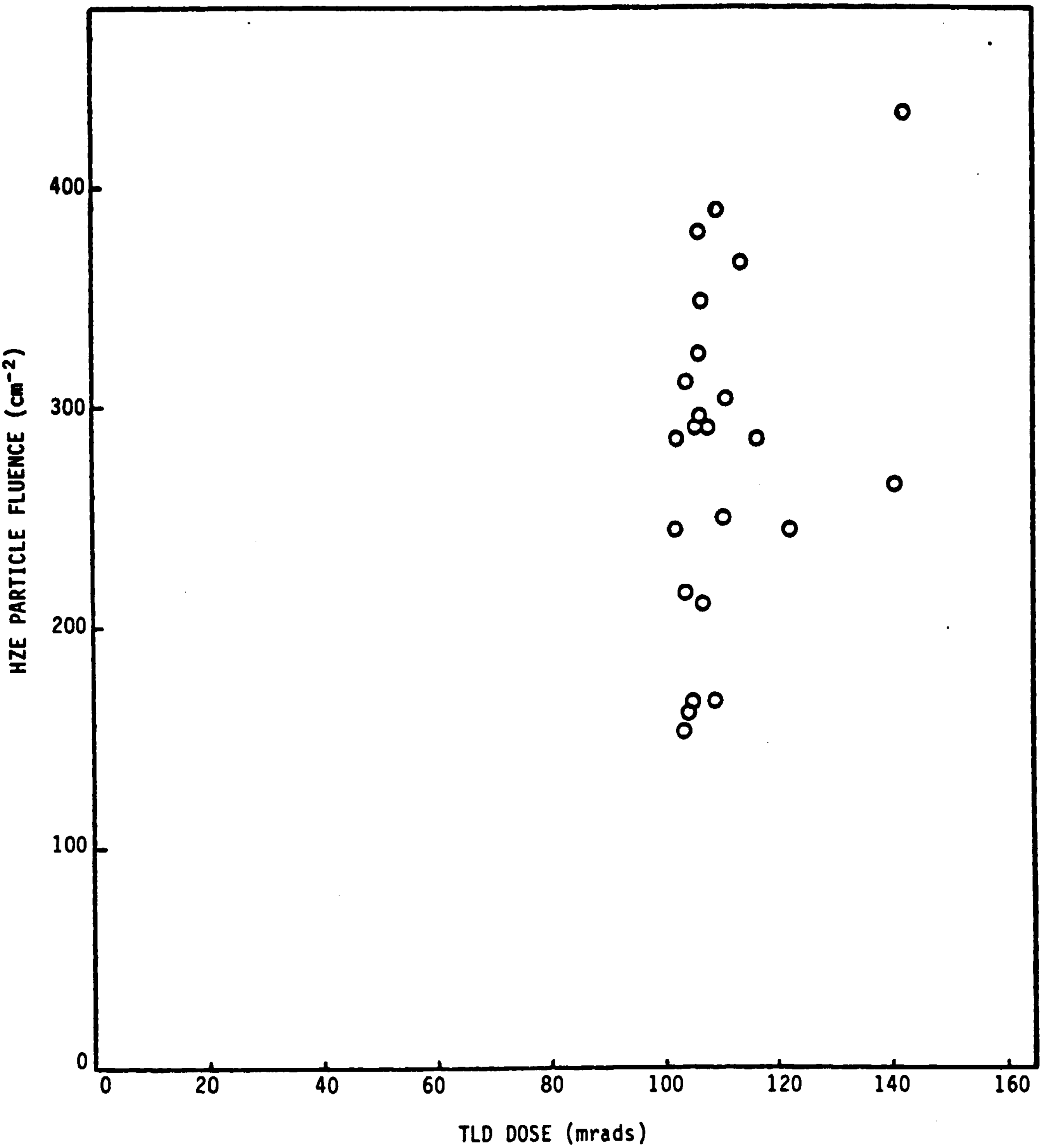

Fig. 3. A plot of the correlation between HZE particle fluences and TLD doses for the PDPs.

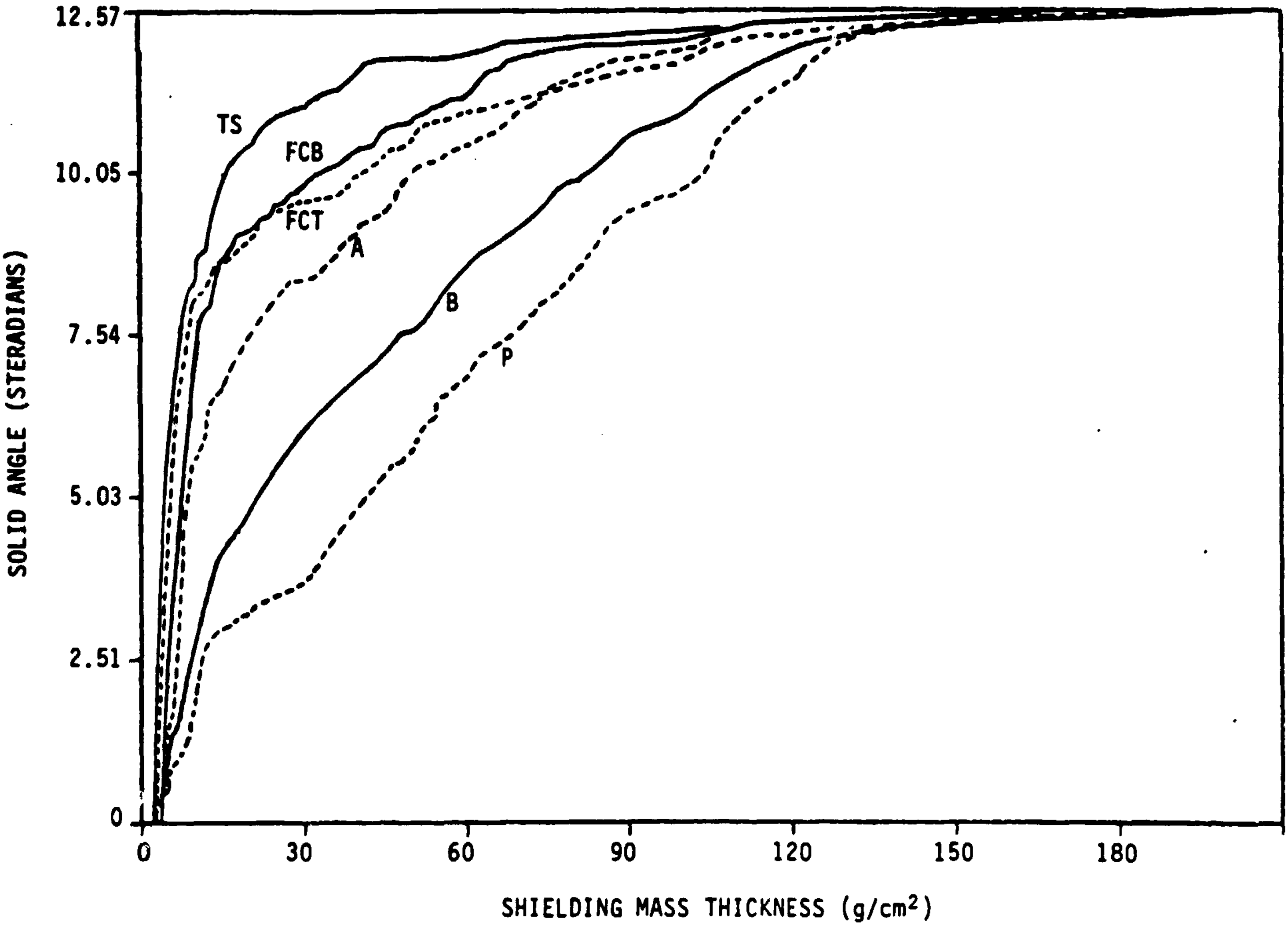

Fig. 4a. Integral angular shielding distributions for several PDP's. The detectors with the higher curves have a greater fraction of total solid angle at smaller values of mass thickness and are therefore more lightly shielded.

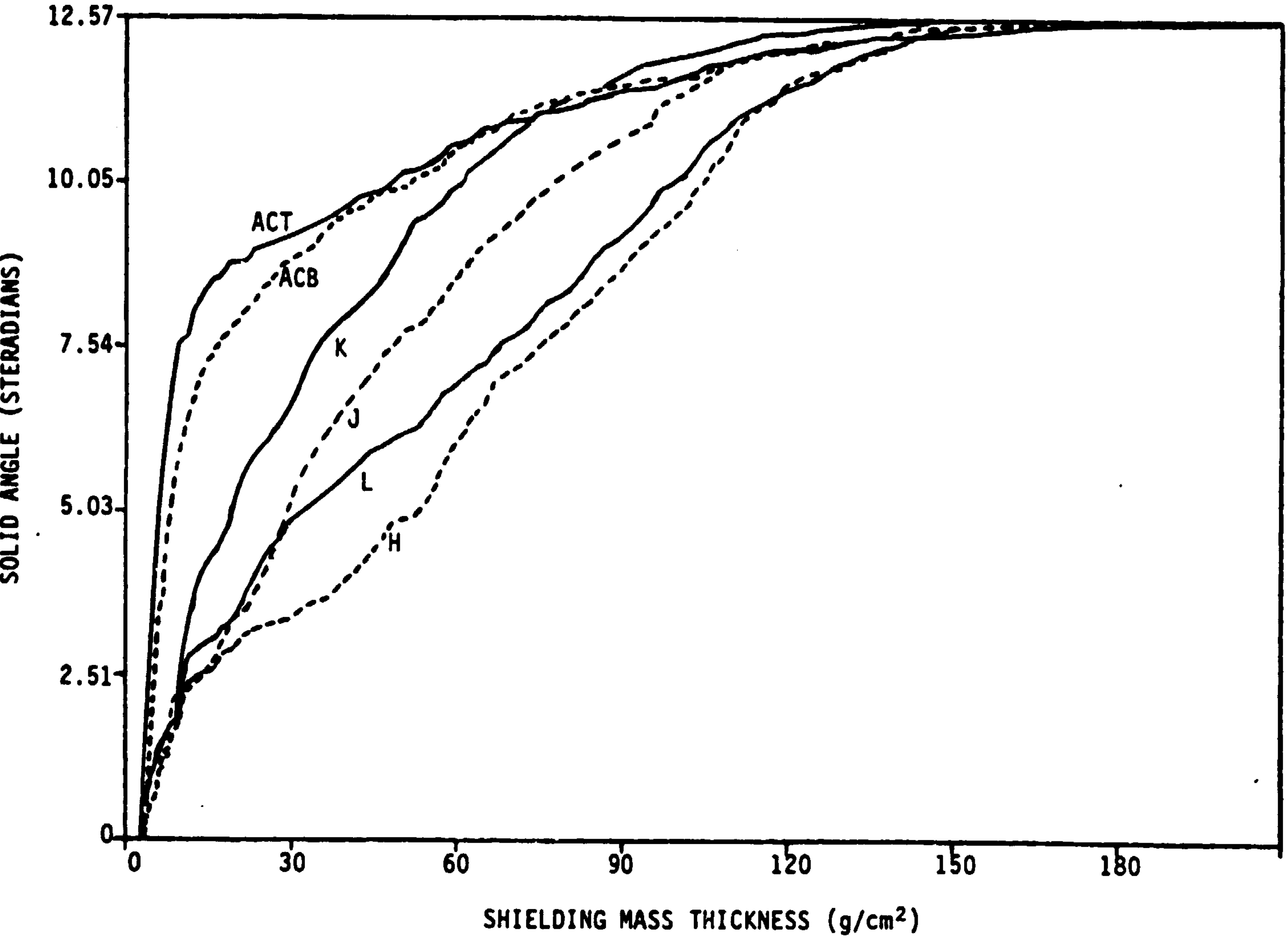

Fig. 4b. Integral angular shielding distributions for several PDP's. The detectors with the higher curves have a greater fraction of total solid angle at smaller values of mass thickness and are therefore more lightly shielded.

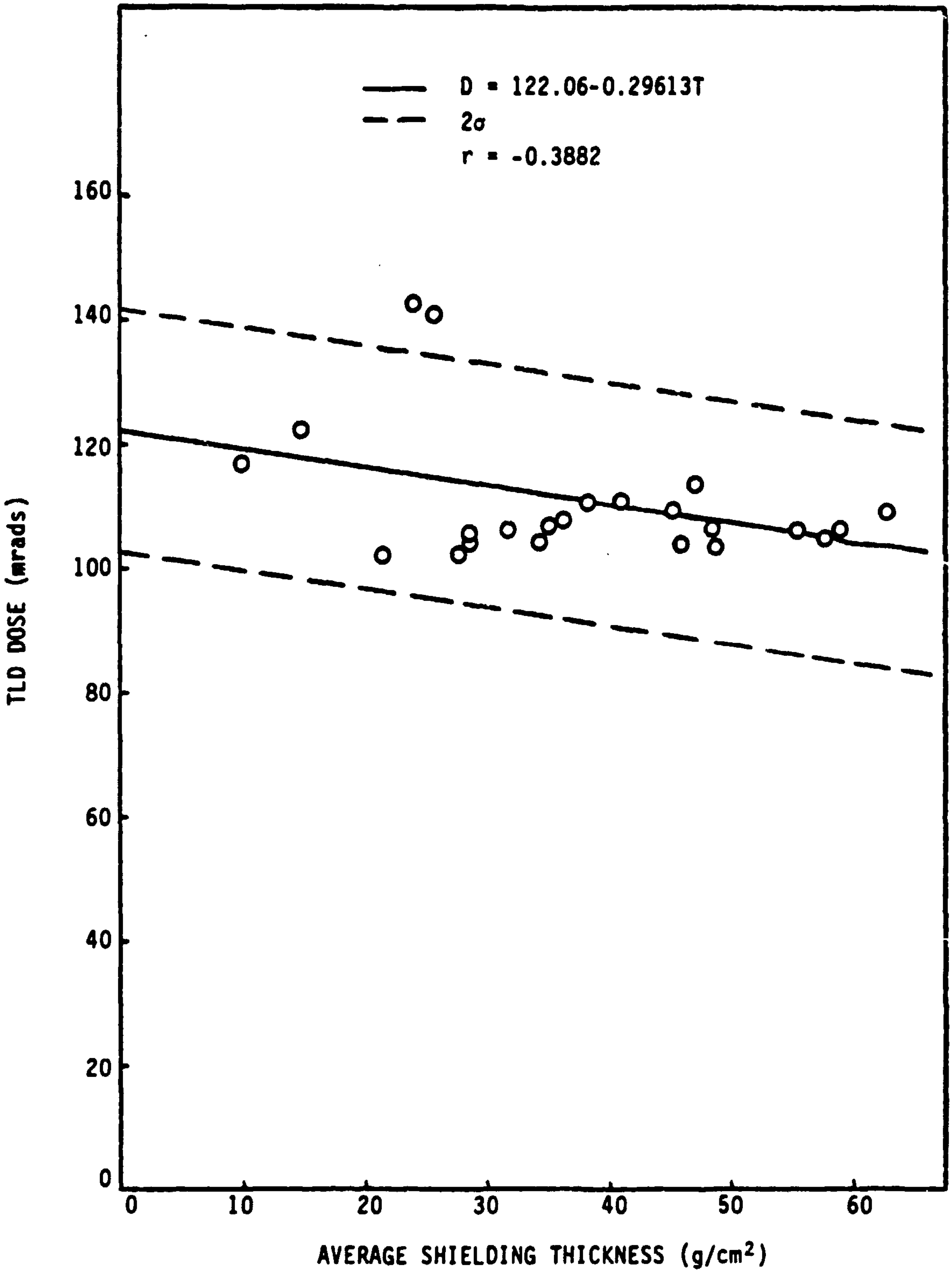

Fig. 5. Variations of the TLD (^{7}LiF) doses with average shielding thicknesses about the PDP's.

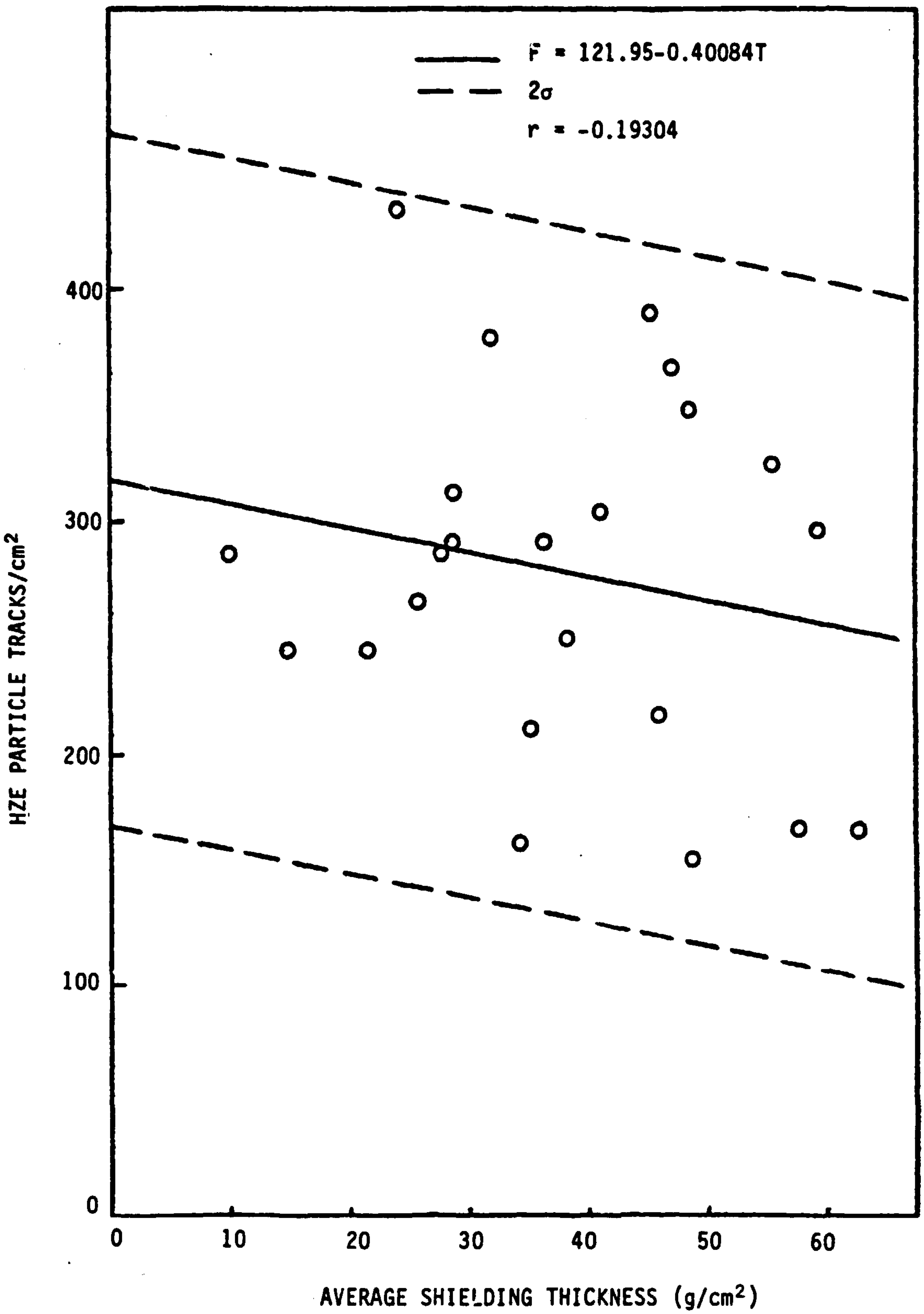

Fig. 6. Variation of the HZE particle fluences with average shielding thicknesses about the PDPs.

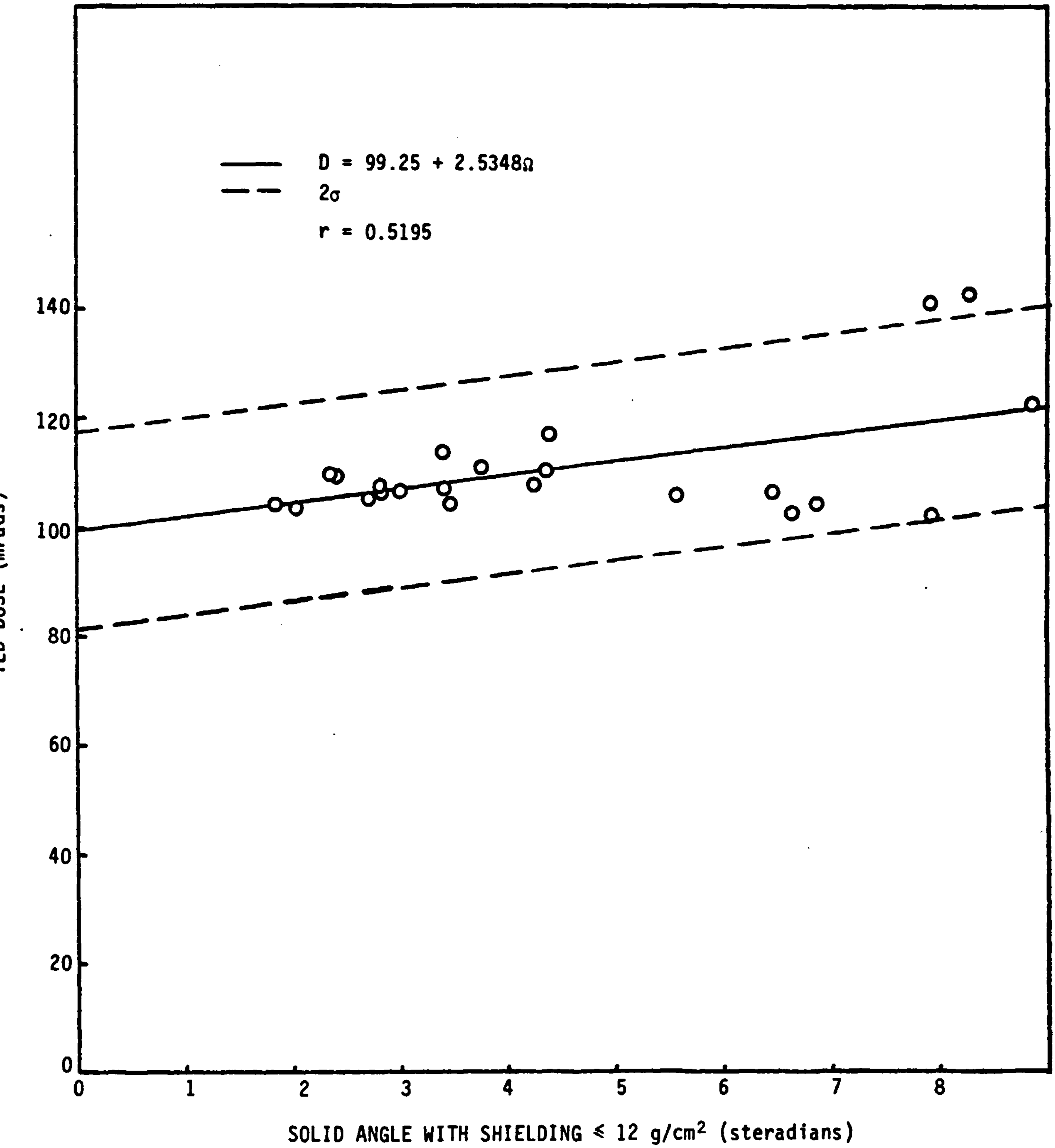

Fig. 7. Variation of TLD doses with the magnitudes of the less shielded (≤ 12 g/cm^2) portions of PDP solid angles.

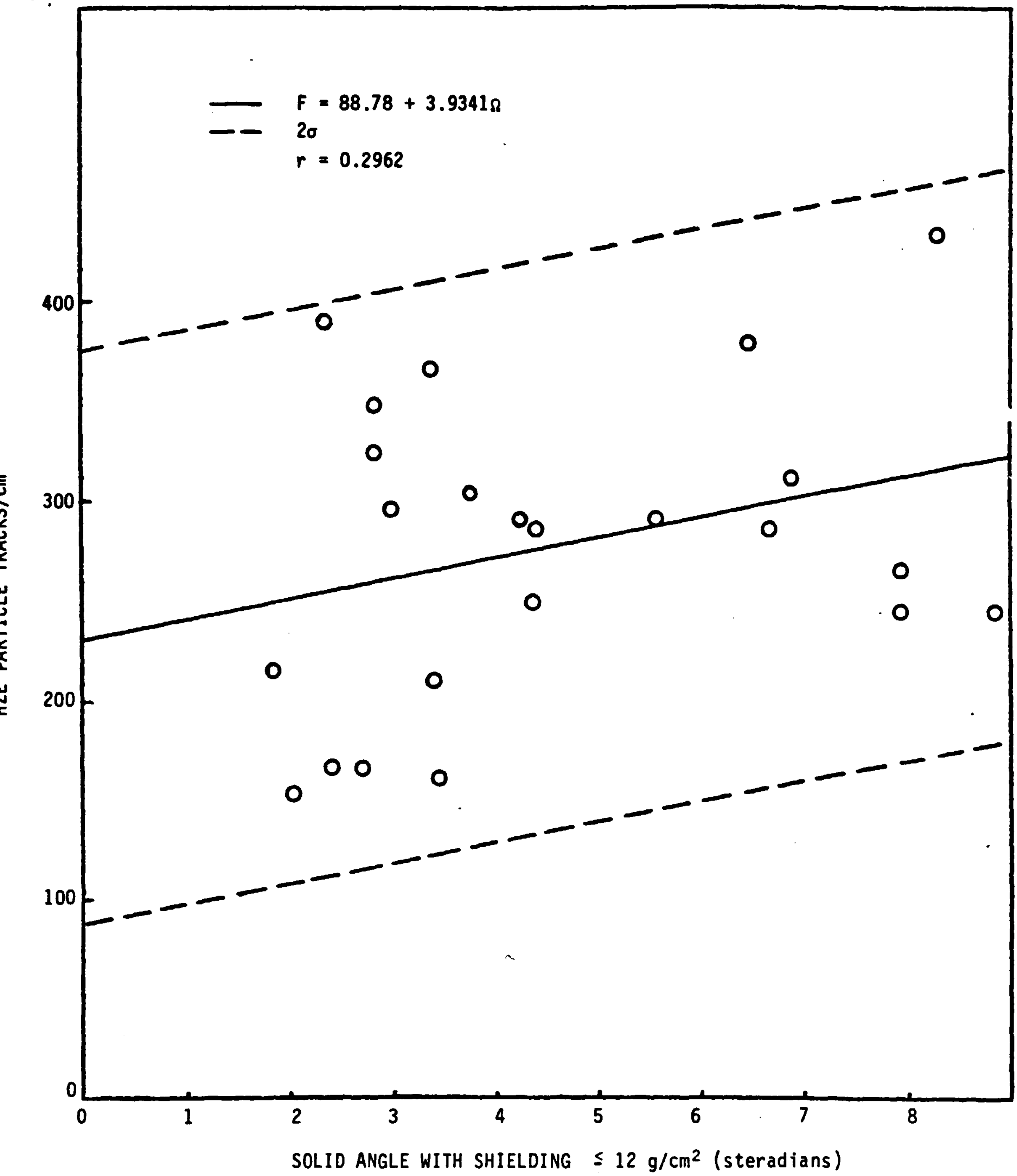

Fig. 8. Variation of HZE track fluences with the magnitudes of the less shielded ($\leq 12\ g/cm^2$) portions of PDP solid angles.

demonstrating shielding effectiveness. In general the greater percentage changes in radiation intensity occur for small shielding thicknesses. The differences in the radiation measurements between the PDP's should therefore be in better correspondence with the lightly shielded portion of solid angle than with another variable such as average shielding thickness. This assumes that the cutoff chosen includes a substantial fraction of total solid angle for most of the detectors. In our case, the included solid angles vary from 1.84 to 8.85 steradians, so that the PDP's are well spread out. As seen from the scatter and correlation coefficients, the improvement in the fitting is small.

Since the CR-39 track detector response is directionally dependent this could be a factor in the large amount of scatter seen in the track fluences. However, when several PDP's having the same angular orientations along the SL-1 starboard and port sides are plotted together in the same manner (Figure 9) the correlation between shielding and HZE track fluences is not improved.

The magnitudes of the TLD and track fluence measurements are seen to be only poorly correlated with the shielding of the PDP's. Factors such as changes in spacecraft orientation with time, directionality of the incident radiation, range-energy relations of the incident particle spectra, etc., are also important to an understanding of the particular radiation levels.

An LET spectrum was generated from a population of particle tracks by measuring the major and minor axes of the eliptical openings of cones where two adjacent tracks formed when the particles passed through the interface of two CR-39 sheets. These measurements were converted to particle LET's by using calibrations of the CR-39 made with accelerated ion beams. The spectrum is plotted against log LET_{200} in Figure 10. The dose rate, RBE and QF of the particles are determined from the LET spectrum.

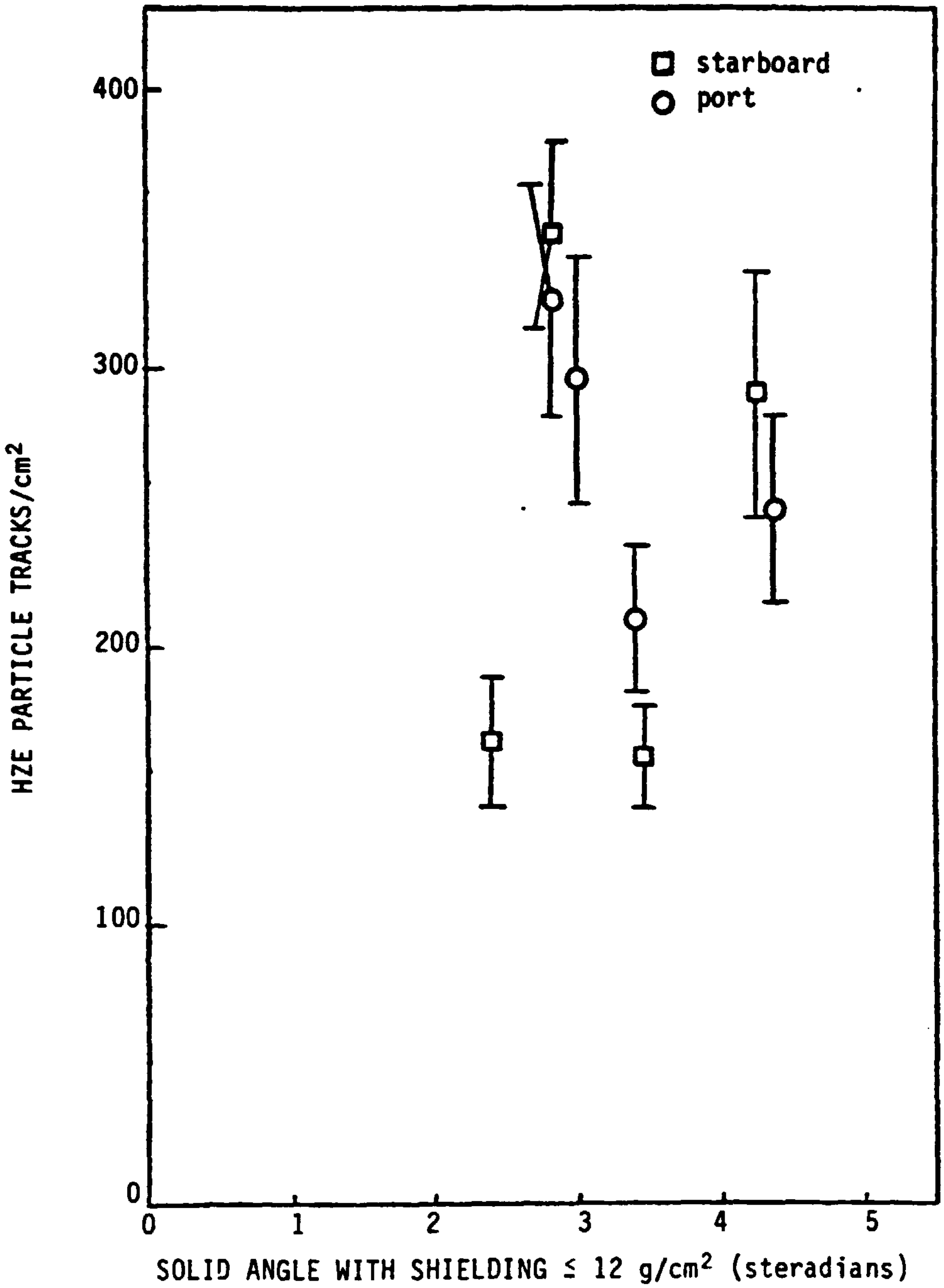

Fig. 9. Variation of HZE track fluences with the magnitudes of the less shielded (≤ 12 g/cm^2) portions of solid angle for several PDP's having the same angular orientations along the starboard and port sides of the SL-1 vehicle.

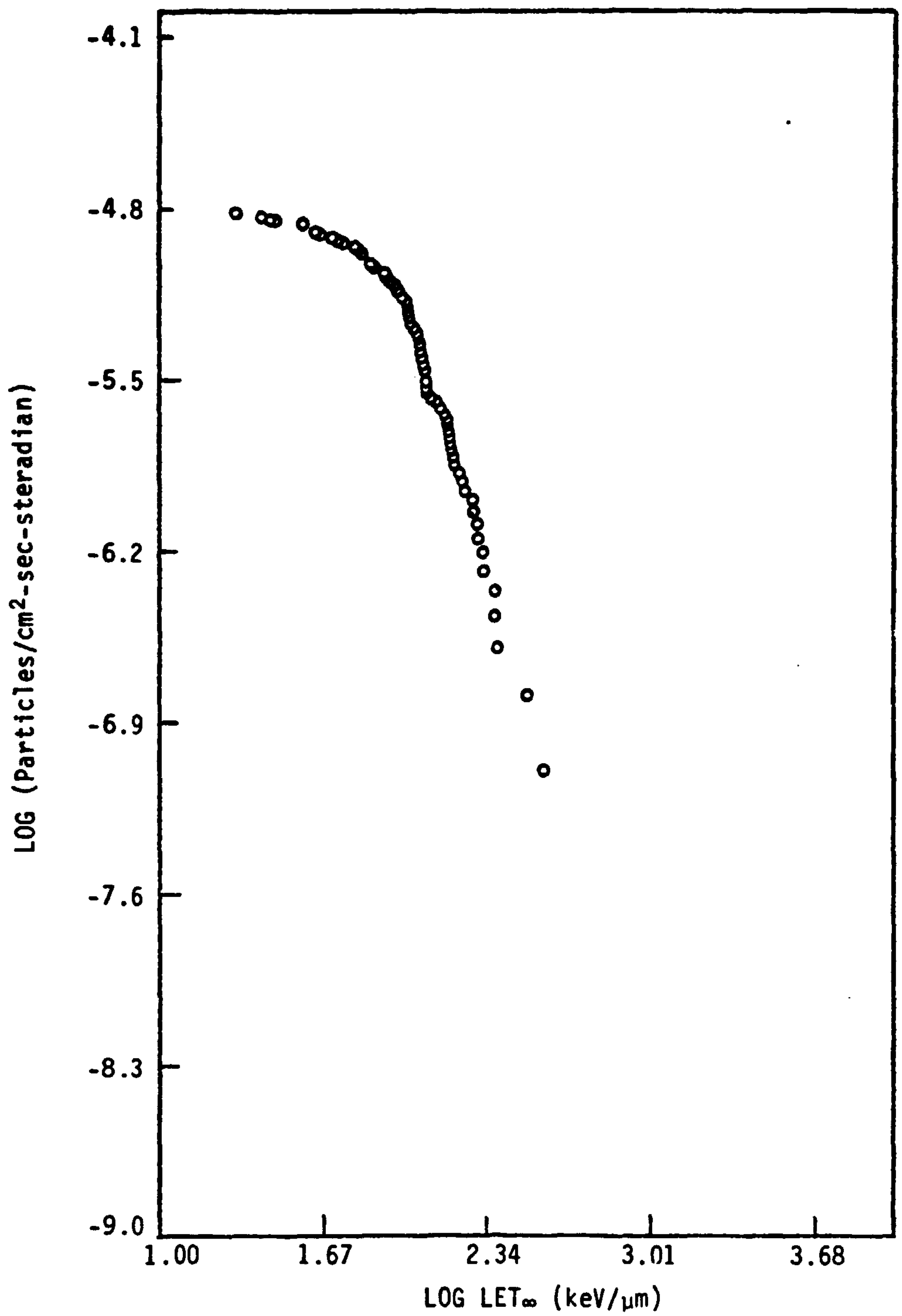

Fig. 10. The LET spectrum of particles measured on Spacelab 1.

The Spacelab 1 spectrum is compared with some other measured and calculated spectra in Figure 11. The earlier measurements were made with Lexan polycarbonate and cellulose nitrate detectors. It is seen that the Spacelab 1 spectrum extends to much lower in LET. This is an advantage of using the more sensitive CR-39 detectors.

The average TLD dose for the detectors listed in Table 1 was 109.8 ± 10.5 mrads. The average track fluence was 278 ± 78 cm^{-2}. This track fluence converts to a dose equivalent of 194 ± 54 mrem, based on the LET spectrum and the relevant RBE values. From a calibration of TLD efficiency versus particle LET it has been calculated that the HZE particles contributed, on the average, 8.6 mrads to the TLD measured dose. The low LET dose measured by the TLD's (QF=1) was therefore 101.2 ± 10.5 mrads. The sum of high and low LET doses, in dose equivalent, is therefore 295 ± 55 mrem. There was an additional dose present, due to neutrons, but this was not measured.

DISCUSSION

The 240-hour STS-9 Shuttle flight was at an orbit of 241 km in altitude with an inclination of 57 degrees. The low LET dose rate in the SL-1 module averaged 10.1 ± 1.1 mrad/day. The dose equivalent rate, neglecting neutrons, was 29.5 ± 5.5 mrem/day. The high LET portion from HZE particles was 19.4 ± 5.4 mrem/day.

A comparison of the radiation dose and dose rate measured on Spacelab 1 and other manned U.S. spaceflights is shown in Table 2 /2/. For low Earth orbit, the effect of a greater orbital inclination (57° for STS-9) is clearly seen as compared with previous flights (28.5°) of the Space Shuttle. Even though STS-9 was at somewhat lower altitude (241 km) than several previous flights (284-297 km),

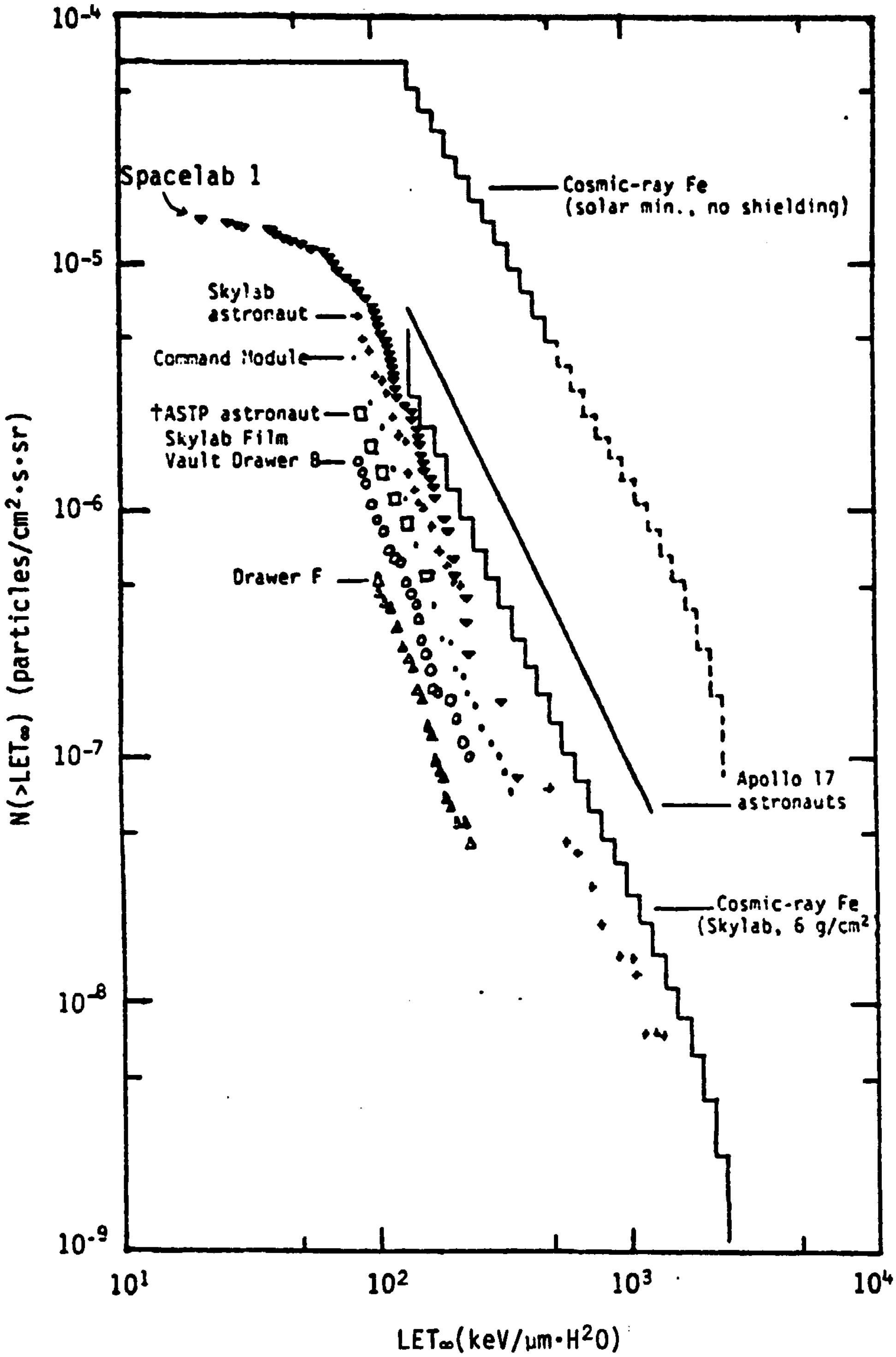

Fig. 11. A comparison of the Spacelab 1 HZE particle LET spectrum with previous measured and calculated spectra. The cosmic-ray Fe spectra were calculated.

TABLE 2. Dosimetry Data from U.S. Manned Spaceflights

Flight	Duration (hrs/days)	Inclination (deg)	Apogee-Perigee (km)	Average Dose (mrad)	Average dose rate (mrad/day)
Gemini 4	97.3 hrs	32.5	296 - 166	46	11
Gemini 6	25.3 hrs	28.9	311 - 283	25	23
Apollo 7*	260.1 hrs			160	15
Apollo 8	147.0 hrs		lunar orbital flight	160	26
Apollo 9	241.0 hrs			200	20
Apollo 10	192.0 hrs		lunar orbital flight	480	60
Apollo 11	194.0 hrs		lunar orbital flight	180	22
Apollo 12	244.5 hrs		lunar orbital flight	580	57
Apollo 13	142.9 hrs		lunar orbital flight	240	40
Apollo 14	216.0 hrs		lunar orbital flight	1140	127
Apollo 15	295.0 hrs		lunar orbital flight	300	24
Apollo 16	265.8 hrs		lunar orbital flight	510	46
Apollo 17	301.8 hrs		lunar orbital flight	550	44
Skylab 2**	28 days	50	altitude ≈ 435	1596	57 ± 3
Skylab 3	59 days	50	" ≈ 435	3835	65 ± 5
Skylab 4	90 days	50	" ≈ 435	7740	86 ± 9
Apollo-Soyuz Test Project	9 days	50	" ≈ 220	106	12
STS-2†	57.5 hrs	38	" ≈ 240	12.5 ± 1.8	5.2
STS-3	194.5 hrs	38	" ≈ 240	52.5 ± 1.8	6.5
STS-4	169.1 hrs	28.5	" ≈ 297	44.6 ± 1.1	6.3
STS-5	120.0 hrs	28.5	" ≈ 297	27.8 ± 2.5	5.6
STS-6	120.0 hrs	28.5	" ≈ 284	27.3 ± 0.9	5.5
STS-7	143.0 hrs	28.5	" ≈ 297	34.8 ± 2.3	5.8
STS-8	70/75 hrs	28.5	" ≈297/222	34.8 ± 1.5	5.8
STS-9	240.0 hrs	57	" ≈ 241	101.1 ± 3.1	10.1
STS-9 (SL-1)				101.2 ±10.5	10.1
STS-41B	191.0 hrs	28.5	" ≈ 297	43.6 ± 1.8	5.5
STS-41C	168.0 hrs	28.5	" ≈ 519	403.0 ±12.0	57.6
STS-41D	145.0	28.5	" 297	42.0 ± 2.8	7.0
STS-41G	29/19/148.5	57.0	" 352/274/224	82.4 ± 2.4	10.0
STS-51A	192	28.5	" 324	94.3 ± 4.9	11.8

*Doses quoted for the Apollo flights are skin TLD doses. The doses to the blood-forming organs are approximately 40% lower than the values measured at the body surface.
**Mean Thermoluminescent dosimeter (TLD) Skylab dose rates from crew dosimeters.
†STS data is an average of USF TLD-700 (^7LiF) readings.

the low LET dose rate is nearly double that previously recorded. The effect is even more dramatic when comparing the dose-equivalent: Spacelab 1 with 29.5 mrem/day as compared with ~10 mrem/day for the previous (28.5° inclination) STS flights. Much of this difference is the result of a substantial increase in the fluences of high LET HZE particles. The Spacelab-1 HZE measurements can also be compared to others made on STS-9, in the crew compartment /11/ and for the VFI /12/ experiment within the SL module. The Spacelab-1 average high LET dose-equivalent of 194 mrem compares with 122 mrem fo the VFI experiment and 76.3 mrem in the crew compartment. These differences reflect the variability of HZE fluences throughout the Space Shuttle.

The strong effect of altitude on dose rate can be observed (Table 2) with Skylab 4 (50°, 435 km) recording $\sim$90 mrad/day. Since some of the future missions of the Spacelab will use similar orbital trajectories, care will have to be taken to protect the parts and experimental equipment which may be sensitive to the radiation encountered. Equipment containing microprocessors such as in life-support systems and computers is susceptible to single-event latchup and soft error upset. The radiobiological effects of HZE particles is, at present, not well understood, but there is growing evidence that they should be treated as single-event phenomena with high quality factors /13/.

Spacelab-1 experiments were designed many years ago. Meanwhile, substantial improvements in the techniques and methods of passive radiation detection have been achieved. For example, the improvements in the plastic track detectors make it possible to extend the LET measurements down into the lower LET range of interest to 4-5 keV/μm. It is also necessary to resolve the problems associated with the knowledge of the shielding in the various locations within the module, so that meaningful intercomparisons with measurements can be made. In addition, further documentation of doses, dose rates, HZE particle fluences, and the contribution from neutrons needs to be documented for other Spacelab orbit altitudes, inclinations and variations caused by changes in the solar cycle and solar activity.

REFERENCES AND NOTES

1. D. M. Rust, Science 216, 939 (1982).

2. E. V. Benton and R. P. Henke, Radiation exposures during spaceflight and their measurement, Adv. Space Res. 3, 171 (1983).

3. J. Janni, A. review of Soviet manned space flight dosimetry results, Aerospace Medicine 40, 1547 (1969).

4. V. Petrov, Y. Akatov, S. Kozlova, V. Markelov, V. Nesterov, V. Redko, L. Smirenny, A. Khortsev and I. Chernikh, The study of the radiation environment in near-Earth space, Space Res. 13, 129 (1975).

5. J. V. Bailey, Dosimetry during space missions, IEEE Trans, Nucl. Sci., NS-23, #4, 1379 (1977).

6. T. M. Jordan, Radiation protection for manned space activities, JPL Publication 83-26, Jet Propulsion Laboratory, Pasadena (1983).

7. E. G. Stassinopoulos, The geostationary radiation environment, J. Spacecraft and Rockets 17, 145 (1980).

8. J. W. Watts, Jr. and J. J. Wright, Charged particle radiation environment for the Spacelab and other missions in low Earth orbit--Revision A. NASA Tech. Memo. TMX-73358, 1-137 (1976).

9. A. Hardy, W. Atwell and R. Beever, NASA-Lyndon B. Johnson Space Center, Houston, Texas; private communication (1984).

10. The LET cut-off of 48 keV/μm for the type of CR-39 used may be refined in the future.

11. E. V. Benton, A. Frank, R. Henke, J. Almasi and R. Cassou, STS-9 Dosimetry Report, TR-62, University of San Francisco (1984).

12. E. V. Benton et al., Radiation measurements with passive detectors for the Spacelab-1 VFI program: Experiment ENVOI, TR-69, University of San Francisco (1985).

13. E. A. Blakely et al., Radiation Research 80, 122 (1979).